Effect of Deformable Baffle on the Mixed Convection of Non-Newtonian Fluids in a Channel-Cavity

Duna T. Yaseen [1,*], Muneer A. Ismael [2]

[1]Department of Mechanical Engineering, Technical Institute/Basrah, Southern Technical University, Basrah, Iraq
[2]Department of Mechanical Engineering, College of Engineering, University of Basrah, Basrah, Iraq
E-mail addresses: duna.yaseen@stu.edu.com , muneerismael@yahoo.com
Received: 11 November 2019; Accepted: 4 December 2019; Published: 2 March 2020

Abstract

A simulation of fluid-structure interaction (FSI) and combined convective heat exchange is accomplished in an open trapezoidal cavity-channel. A non-Newtonian (power law fluid) is inspected within the laminar region. The heat source is simulated by an isothermal hot cavity bottom wall, whereas all the rest solid walls are perfectly insulated. A deformable baffle is fixed at the top wall of the channel and its free end extends towards the open cavity. The location of the deformable baffle on the top wall is varied. The baffle position is investigated together with Richardson number (Ri = 0.01-100) and power law index (n = 0.5-1.5). The problem was solved using finite element method with Arbitrary Lagrangian-Eulerian (ALE) technique. The results are compared with the non-baffled channel. The study shows that the proposed baffled channel enhances the heat transfer notably.

1. Introduction

Complying with the recent developments, researcher's efforts are directed to find new efficient techniques serve in enhancing the convective heat transfer. The natural convection combined with forced convection refers as mixed convection, which plays important role in engineering application such as cooling air has wide range in cooling the computer and electronic devices. The convective heat transfer in channel could be enhanced by using special inserts, cavities, fins and nanofluids. Augmentation of heat exchange in a cavity-channel unit is a main demand owing to its importance in industry and engineering applications. Such a unit is proven to enhance the rate of heat exchange with less pressure drop. Non-Newtonian laminar flow in channels and cavities has drawn some attention in recent years for its crucial advantages of heat transfer development and drag reduction. Combined natural and forced convection of laminar flow of Non-Newtonian fluids is to be investigated for its importance in experimental applications of different modern systems such as food industries [1], blood flow, and paint industries [2]. Heat exchange and streaming flow in a rectangular cavity opened to a parallel-plate channel was simulated by Aminossadati et al. [3]. They used heat source on different positions of the cavity walls. They showed efficient cooling when the heat source is set at the right cavity wall i.e. in opposite to the flow. Islam et al. [4] conducted numerical study of mixed convection in a rectangular channel connected to an open cavity. They used three cases of heat flux location on the cavity wall. Their results showed that, for all cases, the enhancement in heat transfer rate occurs at (H/D = 0.5). Saha et al. [5] numerically investigated mixed convection heat transfer laminar flow in a square lid-driven cavity. They considered the bottom wall of the cavity as sinusoidal surface and fixed at cold temperature, while the top wall moves with a constant velocity and kept at hot temperature. They showed that the heat transfer increase with increase Grashof number and amplitude of bottom wall. The impact of baffle geometry on heat transfer in a rectangular channel was studied by Belmiloud et al. [6]. Their findings clarified that the average number of Nusselt decreases with increasing height of baffles whatever the Nuav takes maximum values for the triangular configuration. Radhakrishnan et al. [7] studied the effect of baffle, which causes increasing heat transfer in a ventilated cavity, and the best position of the baffle among different position was found in which heat transfer rate was enhanced by 50 % as compared to the case of no-baffle. Asif et al. [8] performed a numerical study in a vented cavity including three isothermal baffles. They recorded an enhancement of heat transfer using these baffles. The baffles were placed alternately in the vertical walls. Sripattanapipat and Promvonge [9] considered the impact of different baffle shape, namely diamond-shaped. Two of these baffles were placed on the horizontal walls in a staggered fashion. They found that performance of the flat baffle is lower than that of the diamond baffle for all Reynolds number used. Channel of various aspect ratios and porous baffles were investigated by the following; Ko and Anand [10], Yang and Hwang [11], Yilmaz [12] and Tsay et al. [13]. Feijó et al. [14] implemented the contractual design procedure to study the impact vortex generating by two rectangular hot obstacles mounted alternatively on the channel surfaces. They concluded that the optimum performance is obtained with highest obstacles. Najam et al. [15] assumed fully developed and periodic conditions for longitudinal direction of a channel. They found that for large Reynolds number, fully developed forced flow reduces the

heat transfer notably. Array of three obstacles mounted alternately on the horizontal surfaces of channel was the material of the work of Korichi and Oufer [16]. They addressed some influential aspects of Reynolds number, the obstacle dimensions and position on the heat transfer characteristics. Korichi and Oufer [17] developed the study of [16] for oscillatory flows in the channel over an arrangement of alternating square blocks fixed on the walls. They showed that the upper obstacle lead to increase the heat transfer rate between the blocks and neighboring flow. They reported that larger obstacles augment heat exchange.

Nomenclature	
Ca	Cauchy number
g	Gravitational acceleration (ms^{-2})
E	Dimensional Young's modulus of the fin
p	Dimensionless pressure
k	Thermal conductivity (W/m.K)
Kr	Thermal conductivity ratio
Nu	Local Nusselt number
PEC	Performance enhancement criterion
ds	Dimensionless displacement vector
m	Power-law inconsistency index (kg s m^{-1})
n	Power-law index
Re	Reynolds number
Ri	Richardson number
Pr	Prandtl number
I	Second invariant of the strain tensor rate
T	Temperature (K)
t	Dimensionless time
x, y	Cartesian coordinates (dimensionless)
H	Non-dimensional internal channel height
C_f	Skin friction coefficient
D_h	Hydraulic diameter (m)
f	Friction factor
u	Dimensionless velocity vector
w	Moving coordinate velocity vector (dimensionless)
Greek symbols	
τ	Extra stress tensor (dimensionless)
σ	Stress tensor (dimensionless)
υ	Poisson's ratio
θ	Dimensionless temperature
ψ	Stream function
α	Thermal diffusivity (m^{2}s^{-1})
β	Thermal expansion coefficient (K^{-1})
ε_{ij}	Strain rate = $2(\partial u_i/\partial x_j + \partial u_j/\partial x_i)$
η	Apparent viscosity (kg s m^{-1})
ρ	Density (kg m^3)
Subscripts	
av	Average
c	Cold
h	Hot
in	Inlet
r	Ratio
s	Solid
N	Newtonian
NN	Non-Newtonian Greek symbols
Superscripts	
*	Dimensional parameter

Sun et al. [18] utilized the flow-induced vibration (FIV) resulting from a deformable fin and how it affects the process of convective heat exchange. They studied heat transfer characteristics for different combinations of fin rigidity. They deduced that when the fin shows large-amplitude vibration, the forced convection heat transfer can be augmented notably. Vera and Linan [19] analyzed multilayered, counter flow parallel-plate heat exchangers numerically and theoretically. They established a 2D model to get analytical solutions for the fully developed counter flow in parallel-plate heat exchangers within the laminar region. Kang and Yang [20] simulated the flow and heat transfer process in finned heat exchangers comprising of thin baffles attached on both channel walls periodically. Wang et al. [21, 22] performed many experiments on the heat transfer and pressure drop characteristics of tube heat exchangers containing wavy fin. The mixed convection heat transfer and flow structure in a baffled groove channel was investigated numerically by Sharma et al. [23]. They studied the impact of baffle position and its height. Along with this, the location and height of the baffle on the top wall is varied. Their results showed that the presence of the baffle enhanced the heat transfer.

The fluid-structure interaction (FSI) field is characterized by a complicated flow structure due to the interaction between the moving boundary and the fluid. A violent shear layer is produced along the interface between these media. Such topic is encountered in many recent applications such as piezoelectric fan, membrane industry, bio-medicals and polymer engineering [24]. Abdi et al. [25] conducted thorough numerical study of three different cases to investigate flexible splitter plates for wake control. Single splitter, dual-splitters and tri-splitters were studied. Ghalambaz et al. [26] formulated a convective heat transfer in a cavity including an elastic fin mounted transversely. The fin oscillates by an external force. Their results showed that increasing the non-dimensional amplitude of the oscillating fin enhances the average Nusselt number. They concluded also that the fixed fin augments the heat exchange due to its role in disturbing the fluid flow. Ismael [24] used two alternatives, upstream and downstream baffles acting as vortex generators bound a compliant segment, and found the heat transfer of a certain compliant baffled channel enhances the heat transfer by 94 % compared with non-baffled channel at Re = 250, also he showed that the compliant wall segment lowers the thermal performance of the non-baffled channel. Chakraborty et al. [27] performed experiments in a microchannel compromising a compliant wall segment with externally applied air pressure on the segment. The main conclusion of their study was the possibility of adopting two-dimensional models to describe a three-dimensional system in certain cases. The maximum discrepancy between their experimental (3D) and numerical (2D) results were very low. Non-Newtonian laminar flow in channels has drawn some attention in recent years. This is because its crucial advantages of heat transfer development and drag reduction. Reynolds stress model is described by many failure criteria typically proposed to be related to the pressure sensitivity under various loading conditions by the fluid flow. One of these failure criteria is Von-Misses criteria. Rajesh [28] studied FSI in micro pipe lines to analyze the deformation of the channel walls by fluid flow. He reported that when a flexible obstacle placed at different positions, results in different stress figures. Tanner et al. [29] utilized experimental data to simulate the flow of power-law fluid in

a partially collapsed 2D channel. Compared with Newtonian fluid, they found that the maximal shear rate in deformable tube is about 30 times larger than that in non-deformable tube. Nahar et al. [30] conducted an experimental study on the impact of the cross-sectional area of a collapsible conduit on the rheological properties of Carboxymethyl-cellulose aqueous solution. An external pressure was simulated by immersing the collapsible channel in a water-filled Plexiglas chamber

Thus, today different techniques for enhancing heat transfer in mixed convective flow are focused. In this paper, a 2-D model of mixed convection in power law fluid-structure interaction in an open trapezoidal cavity is developed and solved numerically. The trapezoidal open cavity serves in less thermal and flow resistances and found in some industrial applications such as food processing. The main objective of the present study is to explore the role of a deformable baffle fixed from one end and how the flow and heat transfer alter with the position of this baffle.

2. Mathematical Modeling

Fig. 1 portrays the geometry and coordinates system considered in this study. It consists of a two dimensional open trapezoidal cavity with parallel plates channel. The bottom of the cavity is maintained at hot temperature T_h. Cold fluid of T_c enters the channel with uniform velocity u_{in}. A flexible fin is fixed at the upper wall of the channel and dangles towards the mid of the hot bottom wall of the cavity. The other solid walls are thermally insulated. The fluid is incompressible and non-Newtonian, while the flow is taken within the laminar range. The trapezoidal cavity-channel unit has a baffle of thickness 0.02 H with height H, which is mounted to the top wall of the cavity channel. Fig. 1 (a) shows a baffled cavity-channel unit, while in Fig. 1 (b), a simple cavity-channel with no baffle. The location of the baffle was varied to three different positions; one in the center of the grooved, top wall as shown in Fig. 1 (a), in the left and in the right from the first position (central location). The fluid density is the solely property that assumed to vary with fluid temperature according to Boussinesq's hypothesis, while other properties were assumed constant. The elasticity modulus of the fin is considered not affected by the temperature. The dimensionless unsteady two-dimensional governing equations of continuity, momentum and energy for the power-law fluid which are modeled in the current paper are presented below according to the arbitrary Lagrangian-Eulerian (ALE) method:

$$\frac{\partial u}{\partial x} + \frac{\partial v}{\partial y} = 0 \tag{1}$$

$$\frac{\partial u}{\partial t} + (u - w).\nabla u =$$
$$-\frac{\partial p}{\partial x} + \frac{\eta}{Re}\left(\frac{\partial^2 u}{\partial x^2} + \frac{\partial^2 u}{\partial y^2}\right) + \frac{2}{Re}\left(\varepsilon_{xx}\frac{\partial \eta}{\partial x} + \varepsilon_{yx}\frac{\partial \eta}{\partial y}\right) \tag{2}$$

$$\frac{\partial v}{\partial t} + (u - w).\nabla v =$$
$$-\frac{\partial p}{\partial y} + \frac{\eta}{Re}\left(\frac{\partial^2 v}{\partial x^2} + \frac{\partial^2 v}{\partial y^2}\right) + \frac{2}{Re}\left(\varepsilon_{yy}\frac{\partial \eta}{\partial y} + \varepsilon_{xy}\frac{\partial \eta}{\partial x}\right) + Ri.\theta \tag{3}$$

$$\frac{\partial \theta}{\partial t} + (u - w).\nabla \theta = \frac{1}{Re.Pr}\left(\frac{\partial^2 \theta}{\partial x^2} + \frac{\partial^2 \theta}{\partial y^2}\right) \tag{4}$$

For elastic baffle;

$$\frac{Ca}{\rho_r}\frac{d^2 d_s}{dt^2} - \nabla\sigma = 0 \tag{5}$$

$$\frac{\partial \theta}{\partial t} = \alpha_r \nabla^2 \theta \tag{6}$$

Where, u and w are the velocity vector and the moving coordinate, respectively. p is the fluid pressure, θ is the fluid or solid temperature, σ is the stress tensor, which exerts on the deformable baffle due to the fluid flow pressure, ds is the baffle displacement vector, α_s is the thermal diffusivity of solid, α_f is the thermal diffusivity of fluid, β is the thermal expansion coefficient, $\rho_r = \frac{\rho_f}{\rho_s}$ is the density ratio, and $\alpha_r = \frac{\alpha_s}{\alpha_f}$ is thermal diffusivity ratio.

Most non-Newtonian fluids in practice follow the power-law model, which is mentioned as;

$$\eta = m\left(\frac{I}{2}\right)^{n-1/2} \tag{7}$$

Where, $\frac{I}{2} = 2(\frac{\partial u}{\partial x})^2 + 2(\frac{\partial v}{\partial y})^2 + (\frac{\partial u}{\partial y} + \frac{\partial v}{\partial x})^2$, η is the viscosity, which is considered to be a function of the shear rate.

The dimensionless groups appearing in the above equations are defined as follows;

$\theta = \frac{T-T_c}{T_h-T_c}$ is the dimensionless temperature, $Re = \frac{\rho u_{in}^{2-n} H^n}{m}$ is the Reynold number, $Ri = \frac{g\beta\Delta T H}{u_{in}^2}$ is the Richardson number, $Pr = \frac{v_f}{\alpha} = \frac{\eta c_p}{k} = \frac{c_p m}{k}\left(\frac{u_{in}}{H}\right)^{n-1}$ is the prandtl number, $Ca = \frac{\rho_f u_{in}^2}{E}$ is the caughy number where E is the modulus of elasticity of the baffle, ν is the Poisson's ratio.
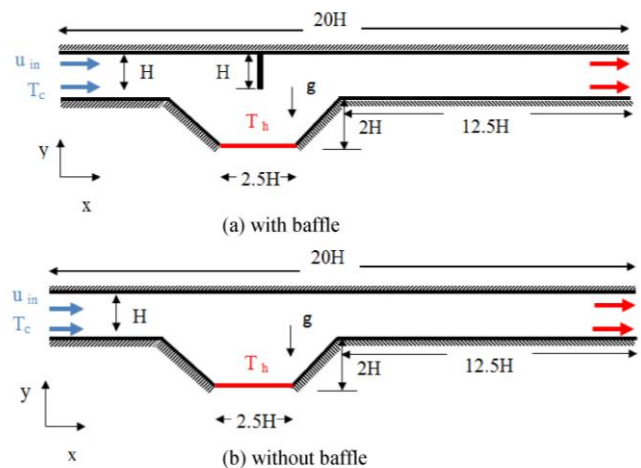

Fig. 1 Physical description of mixed convection in cavity channel.

For no-slip boundary condition over the baffle surface, the stream function is calculated as $u = \partial\psi/\partial y$ and $v = -\partial\psi/\partial x$.

The dimensionless initial and boundary conditions are as follows;
1. At channel inlet, $u = 1$, $v = 0$, $\theta = 0$.
2. At channel outlet, $p = 0$, $v = 0$, $\partial u/\partial x = 0$, $\partial\theta/\partial x$.
3. At the bottom wall of the cavity (hot wall), $\theta = 1$.
4. At adiabatic walls, $\partial\theta/\partial n = 0$.

For the fluid- solid interface, $u = 0$, $\frac{\partial \theta_f}{\partial n} = k_r \ \frac{\partial \theta_s}{\partial n}$,

Where, $k_r = \frac{k_s}{k_f}$ is the thermal conductivity ratio, k_f and k_s are the thermal conductivity of fluid and solid, respectively. We used $k_s = 10 \ k_f$.

For FSI, the pressure and fluid force acting on the baffle. For no-slip boundary condition for the fluid at the baffle interface results in:

$$\frac{\partial d_s}{\partial t} = u \tag{8}$$

And

$$\frac{1}{Ca}\sigma . n = -p + \frac{1}{Re}\left(\frac{I}{2}\right)^{n-\frac{1}{2}}\left(\frac{\partial ui}{\partial x_j} + \frac{\partial u_j}{\partial x_i}\right) \tag{9}$$

The initial conditions are (at $t = 0$): $\theta = 0$, $u = 0$ and $P = 0$.

To evaluate the heat transfer between the bottom groove walls and the fluid, the Nusselt number is used. Considering the continuity of the heat transfer, this dimensionless number can be defined as:

$$Nu = -\left(\frac{\partial \theta_f}{\partial n}\right) \tag{10}$$

$$Nu(t)_{av} = \frac{1}{2H/H}\int_0^{\frac{2H}{H}} \left(\frac{\partial \theta_f}{\partial y}\right)dx \tag{11}$$

Due to the continuous oscillation of the baffle (fluttering), the average Nusselt number is averaged again over the steady state time (t_s):

$$Nu_{av} = \frac{1}{t_s}\int_0^{t_s} Nu(t)_{av} \ dt \tag{12}$$

The physical quantities of interest in this problem are the skin friction coefficient and the Nusselt number, which are defined as [18]:

$$C_f = \frac{\tau_w}{\rho u_{in}^2} \tag{13}$$

Where, τ_w is the shear stress.

In order to judge the overall performance of the process of heat transfer in the present problem, it is important to calculate a comprehensive criterion. This criterion is a dimensionless term and takes into account the process of the heat transfer and the produced pressure drop through the entire channel. By this criterion, it is possible to inspect the impact of geometrical parameters under different flow conditions:

$$PEC = (Nu_{av}/Nu_o)/(f/f_o)^{\frac{1}{3}} \tag{14}$$

Where, the subscript "o" stands for the non-baffled channel. The mechanical performance can be evaluated in terms of flow resistance factor (f) as a ratio of wall shear stress to kinetic energy of the flow. The friction factor was estimated from the pressure drop values using the following equation:

$$f = \frac{2\Delta p^* D_h}{\rho u_{in}^2 L} \tag{15}$$

Where, ρ is the fluid density, Δp^* is the dimensional pressure drop, D_h is the hydraulic diameter ($D_h = 2H$) and $L = 20H$ is the length of the channel. The dimensionless pressure drop is obtained from $\Delta p = \Delta p^*/\rho u_{in}^2$.

$$\Delta p = P_{out} - P_{in} \tag{16}$$

$$f = \frac{\Delta p}{5} \tag{17}$$

The performance evaluation criteria (PEC) were calculated by Eq. (14). Noticeably, PEC >1 means that the heat transfer enhancement is drastically larger than pressure drop.

3. Numerical Analysis

3.1. Numerical procedure

FSI is introduced to enhance the heat transfer and thermal stress individually. Navier-Stokes equation was implemented to represent the momentum exchange between the fluid and the deformable baffle. To deal with FSI modeling, the arbitrary Lagrangian-Eulerian (ALE) method based on finite element method has been adopted to get approximated numerical solution of the governing equations (1) to (6). These equations have been transformed to the weak form and discretized according to the Galerkin finite element method [31]. With this method, the movement of mesh arising from the oscillation of the fin is considered robustly. The suitable step of time is chosen based on the following criterion.

$$\Delta t^* \leq \frac{1}{2}\frac{(\Delta x)^2}{\alpha} \tag{18}$$

Where, Δx is the dimensional distance between nodes in the computational grid, α stands for says the thermal diffusivity of the fluid. It is worth noting that the choice of Δt should be related with the mesh of the numerical solution. Since the present study is dimensionless, relation (18) is modified to be dimensionless as to be:

$$\Delta t = \frac{\Delta t^* u_{in}}{H} \tag{19}$$

The grid mesh of the present computational domain is achieved by applying finer grid. A criterion error of 10-3 is set to stop the computations.

The criterion of convergence of the numerical solution is based on the following relative error formula:

$$\left|\frac{\Gamma^{i+1} - \Gamma^i}{\Gamma^{i+1}}\right| \leq 10^{-3} \tag{20}$$

Where, i stand for the iteration number and Γ for velocity, pressure or temperature.

3.2. Grid independence test

The mesh dependency test has been carried out for conditions that are expected to produce strongest flow situations namely, shear thinning fluid (power index n is lower than unity) and higher Richardson number. As presented in Table 1 and Fig. 2 (a), an acceptable accuracy and economic elements led us to adopt the mesh grid of 29207, which is shown in Fig. 2 (b). Following on constraint (18), the step of time decreases with increasing grid size, thereby, the suitable time step of 29207 elements was found to be 0.1. The element type is unstructured triangular element. This mesh was adopted throughout the current paper after confirming it with other numerical and experimental results. The confirmation was achieved with experimental 3D geometry of Chakraborty [27], which is approximated to 2D geometry. These comparisons have been considered as Newtonian two-dimensional model of the experimental setup illustrated in Fig. 3 (a). It was proven that 2D models can be used to describe a 3D system in case the width of the channel (and consequently the width of the flexible membrane) is ($W > 2L$). Fig. 3 (b) depicts reasonable agreements between present results and the corresponding normalized data for two magnitudes of the average input velocity. Thereby, the reliability of the numerical solution and be relayed on.

Table 1 Grid independent study for Re = 100, Ri = 100, n = 0.5 and Ca = 10^{-4}.

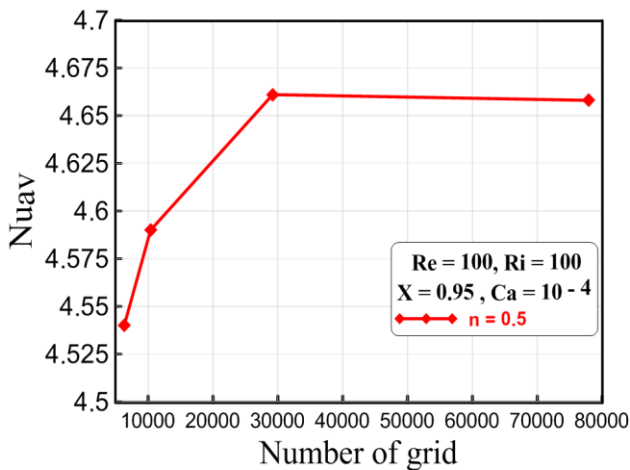| Number of elements	Nu_{av}	|Percentage Error|
6314	4.54	-
10377	4.58	0.873
29207	4.661	1.738
77878	4.658	0.064

Fig. 2 (a) Grid independent study for Re = 100, Ri = 100, n = 0.5 and Ca = 10^{-4}.
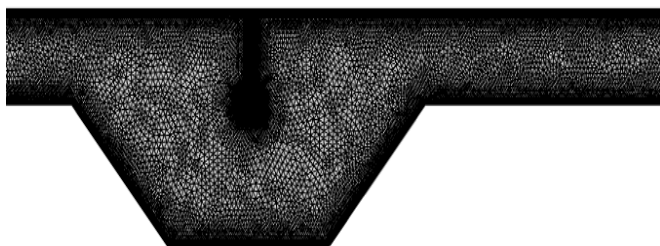

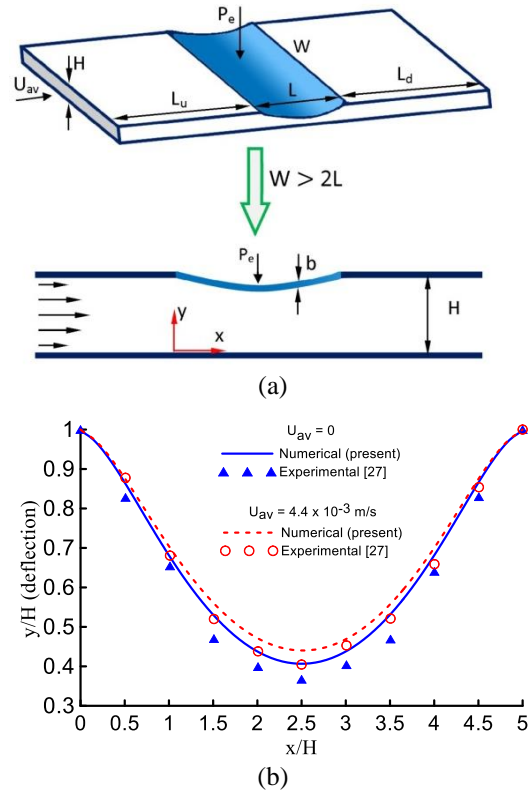**Fig. 2 (b)** Mesh used in the current study.

Fig. 3 Comparison with experimental data, **(a)** experimental 3D geometry of Chakraborty et al. [27] and its approximated 2D geometry, **(b)** comparison of membrane normalized deflection for U_{av} = 0 and 4.4 × 10^{-3} m/s, the other parameters are Pe = 8 kPa, b = 60 μm, H = 200 μm, W = 3 × 10^3 μm, L = 1 × 10^3 μm, L_u = 14 × 10^3, L_d = 14 × 10^3 μm.

4. Results and Discussion

The present study has been carried out in mixed convection laminar regime where Ri varies from 0.01 to 100 and different power law indices n (0.5 - 1.5) with different locations of the deformable baffle. Reynolds and Prandtl numbers have been fixed at 100 and 1, respectively. Cauchy number which represents the ratio of inertial force to elasticity force is fixed at 10^{-4}.

4.1. Time dependent results

Results with time are studied for two sakes, the first is to follow the deformation of the baffle and the second is to inspect the time at which the results reach steady state. For this purpose, the time dependent average Nusselt number has been followed with time (0.1 time step) up to final time of 100. Fig. 4 tell us that almost after t = 5, the average Nusselt number becomes independent of time and this give us an indication to that the deformable baffle has kept its fixed deformed shape. However, for more ascertain, the shape of the baffle together with the streamlines and isotherms have been figured out in Fig. 5. The figure ascertain that after t = 5, the deformed baffle still stressed in a fixed shape due to the circulation of fluid behind it. The fluid circulates in three districts zones, in front and behind baffle and at the entrance of the downstream channel. The fluid circulation behind the baffle is strong enough to push the baffle and bends it in the pattern shown in Fig. 5. Regarding the patterns of contours and the baffle shape, there are no considerable differences between the times t = 5 and 19, as such, the time at which the results are presented in the forthcoming sections is t = 19. This decision was made because Figs. 4 and 5 were drawn at parameters leading to strong flow and heat transfer (Re = 100, Ri = 100 and n = 0.5).
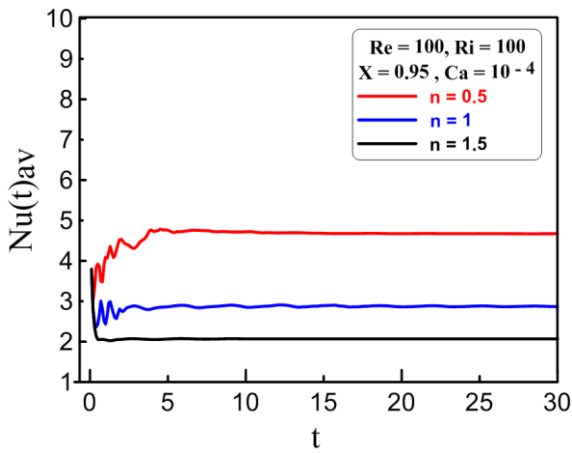
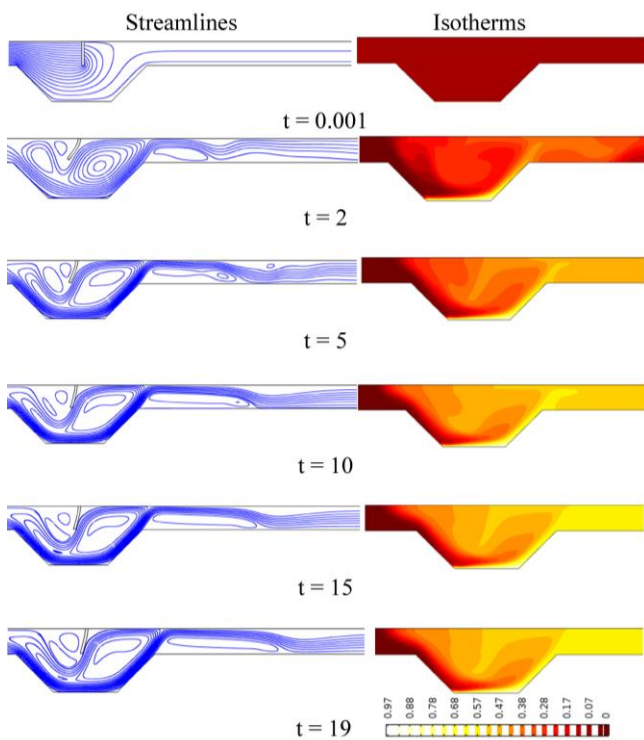**Fig. 4** Average Nusselt vs. time for Re = 100, Ca = 10^{-4}, and Ri = 100.

Fig. 5 Baffle deformation, streamlines and isotherms for different values of t at Ri = 100, central baffle location (X = 0.95) and n = 0.5.

4.2. Effect of power-law index

The value of power-law index implies to the extent by which the fluid viscosity increases with shear rate (shear thickening fluid, n > 1), decreases with shear rate (shear thinning fluid, n < 1) or remains invariant (Newtonian fluid n = 1). Fig. 6 presents the variations of baffle shape, streamlines and isotherms with n for Ri = 100 and central baffle (X = 0.95). For (n = 0.5), the viscosity of fluid decreases with velocity gradients, therefore, the viscous force becomes lower within the zones of high velocity gradients underneath the baffle, for example. This resulting in multi-secondary flows, thus the recirculation of fluid behind the baffle pushes it to bend backward. When n = 1, the viscosity becomes irrespective of shear rate, therefore, flow bifurcations are reduced and a main circulation underneath the baffle bends it backward. For n = 1.5, the viscous force increases within the zone of high velocity gradient, therefore only small vortex behind the baffle can be observed and this vortex is insufficient to make notable deformation on the baffle.

The contours of the isotherms show that the output fluid is hotter with lower n and vice versa as shown in the exit channel downstream the cavity. This mean that at Ri = 100, the heat removed from the heated segment is greater for lower n. Fig. 7 supports this fact where the average Nusselt number has greatest value when n = 0.5 and lowest value at n = 1.5. However, when Ri ≤ 10, the shear thinning fluid experiences lowest Nusselt values. This may be referred to that when the buoyancy force relatively decreases, the fluid bifurcation acts to block the convective heat transfer and then decreasing Nusselt number.
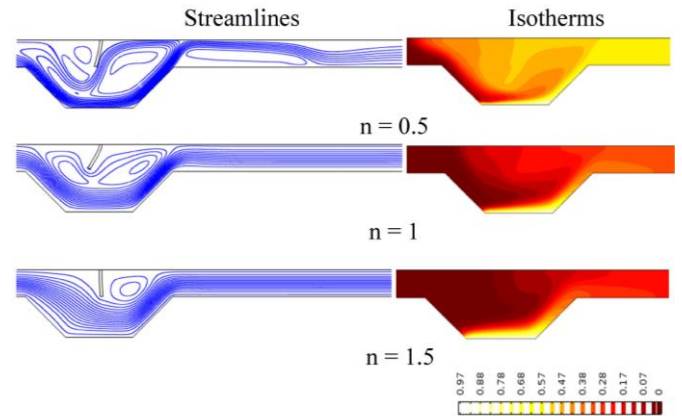

Fig. 6 Baffle deformation, streamlines and isotherms for different values of n at Ri = 100 and central baffle location (X = 0.95).
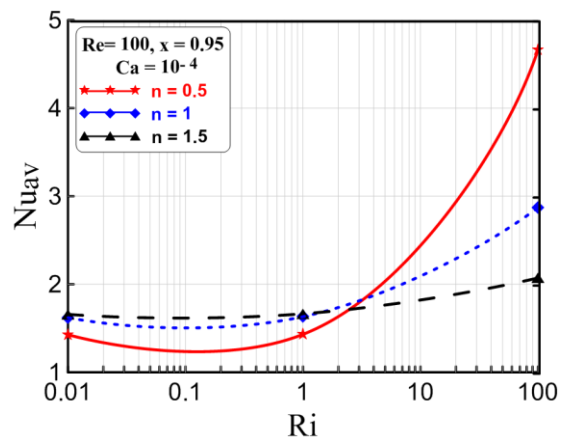

Fig. 7 The average Nusselt vs. Richardson number for different power law indices.

4.3. Effect of Richardson number

The impact of Richardson number on the baffle deformation, streamlines and isotherms is shown in Fig. 8 for n = 0.5 and central baffle location (X = 0.95). The streamlines and the baffle deformation are invariant with Ri up to Ri = 10. The solely weak circulation behind the baffle propagates slightly with Ri and resulting in bending the baffle in forward sense due to the impact of the fresh air entering the channel. Despite increasing Ri from 0.1 to 10, which strengthens the buoyancy force, the patterns of the temperature contours imply to that the temperature gradient occurs mainly close to the heat source. Far from the heat source, stratification isotherms indicate to convective heat transfer. When Ri = 100, appreciable bifurcation and circulation are observed in the streamlines resulting in forward bending of the baffle. These bifurcation and circulation contribute in efficient flow mixing which can be characterized by random isotherms and hotter fluid in the

channel exit. The hotter fluid means quantitative heat removal from the source.

4.4. Effect of the baffle location

The impact of the geometrical parameter, namely the location of the baffle for Ri = 100 and n = 0.5 is analyzed in this section. Three locations of Fig. 9 have been inspected: left, center and right with respect to the cavity center. The dimensionless distances between these locations and the channel inlet are X = 0.75 (left), 0.95 (centered) and 1.1 (right). The left location is nearer to the inlet part of the channel, thus the flow enters the cavity directly and moves intensively along the bottom and sidewalls of the cavity. Behind the baffle, a main recirculation is formed and pushes the baffle forward. Another elongated recirculation is formed in the inlet of the exit channel part. When the baffle is located opposite to the center of the cavity, the available space will permit to form the bifurcations and secondary flow recirculation. On the other hand, the space behind baffle shrinks and leads to weaken the fluid circulation. The right location brings the baffle to be narrower to the inlet of exit channel part. Consequently, more and more space will be available before the baffle resulting in enhancing the bifurcation and extending the circulation. Contrarily, the space behind the baffle gets more shrink. Generally, the recirculation formed in the exit channel part does not influenced by the location of the baffle. The distribution of the isotherms of the left location depicts notable temperature gradients within the cavity because the fresh fluid is forced to pass over the hot wall and thus conveys more heat transfer. Although other locations present random isotherms, the fluid within the exit channel part looks with the same hot temperature for all baffle locations, the behavior noticed in the streamlines. The average Nusselt number for the three locations altogether with free channel (no baffle) is inspected for n = 0.5 and 1.5 and different Richardson number is shown in Fig. 10 (a) and (b), respectively. The figure displays that the left location gives the largest Nusselt number for all n's and Ri's. This is due to fluid path created by this location which directs the fresh fluid towards the heat source. When the baffle location becomes far from the inlet part of the channel, the flow finds roomy free path away from the heat source, thus less heat exchange occurs. Therefore, Nusselt number decreases with far baffle locations. This figure also shows the role of the baffle in enhancing the convective heat transfer, where the free channel experiences the lowest Nusselt number.
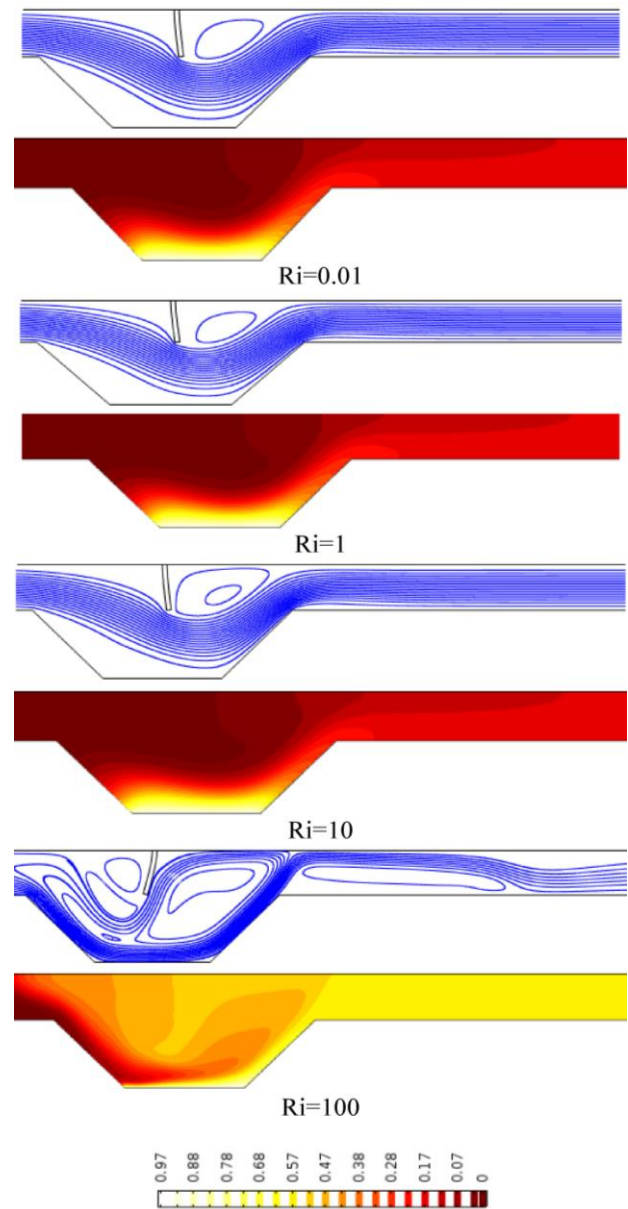

Fig. 8 Baffle deformation, streamlines and isotherms for different values of Ri at n = 0.5 and central baffle (X = 0.95).

4.5. Thermal performance

To make a decision about the best performance should not be based only on the Nusselt number. The hydraulic pressure drop should be taken into account because the high pressure drop requires larger pumping power. The thermal performance criterion (PEC) mentioned in equation (16) fulfills this issue. Figure 11 depicts that the best thermal-hydraulic performance can be attained when the baffle is located in the left of the cavity center i.e. close to the exit of the inlet channel part. This means that the augmentation of the average Nusselt number overcome the losses resulting from the pressure drop along the channel. However, the figure shows that the performance criterion decreases with increasing Richardson number. This implies to that although the higher Richardson number increases the Nusselt number, the generated strong circulations and bifurcations result in higher pressure drop.
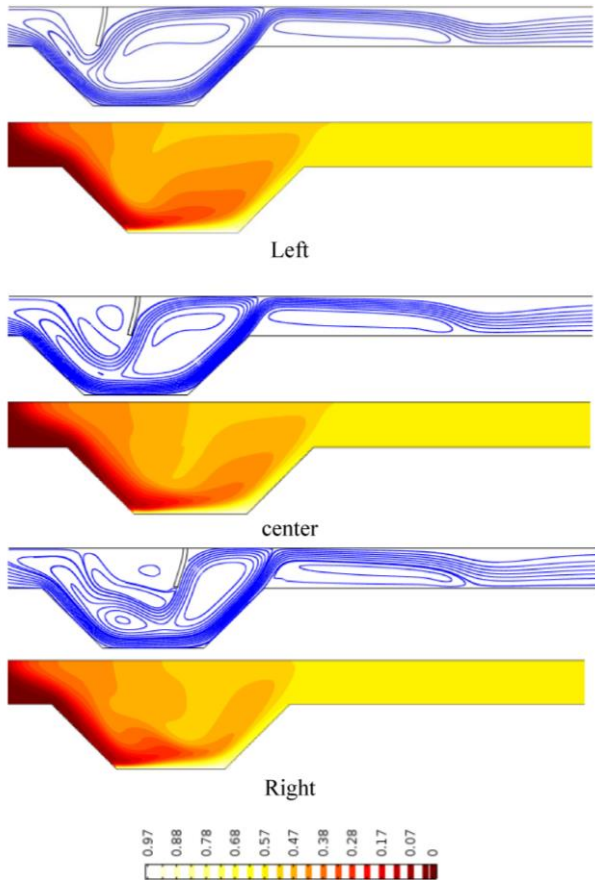
Fig. 9 Baffle deformation, streamlines and isotherms with different baffle locations at Ri = 100 and n = 0. 5.
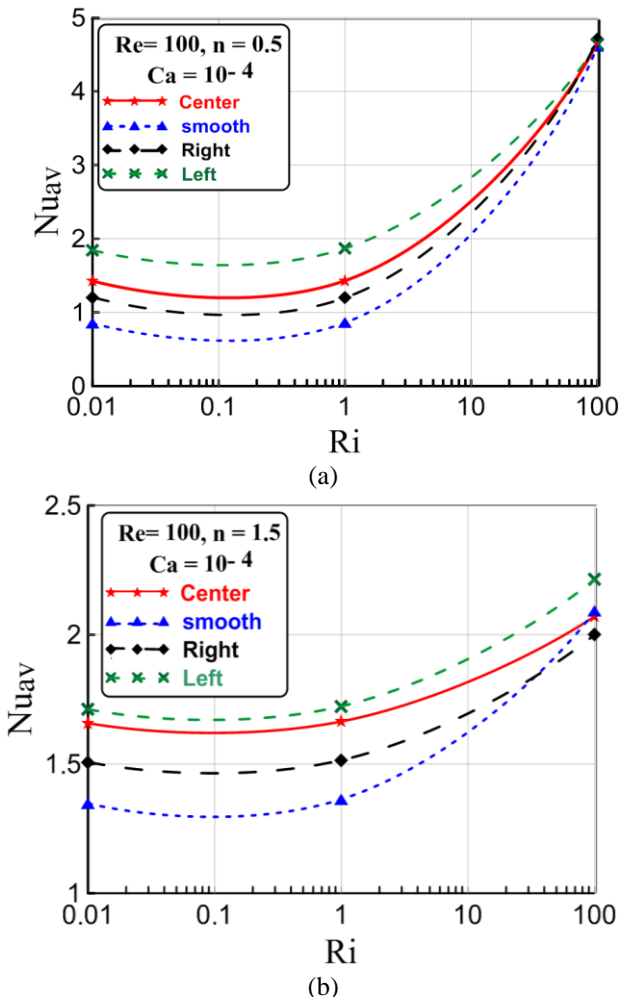

(a)

(b)

Fig. 10 The average Nusselt number vs. Richardson number for different baffle locations for **(a)** n = 0.5 and **(b)** n = 1.5.
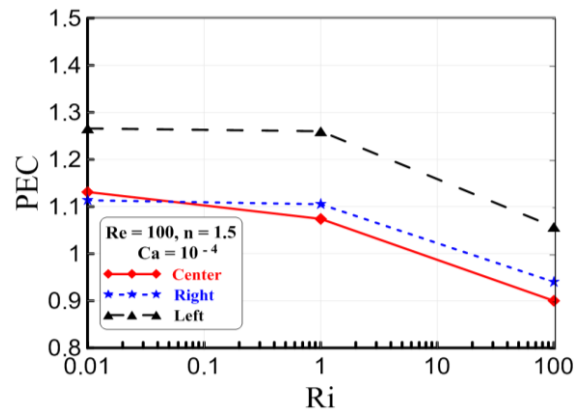

Fig. 11 Thermal-hydraulic performance criterion with Richardson number and baffle location for n = 1.5.

5. Conclusions

A numerical study of power law fluid-structure interaction in a trapezoidal cavity opened to a rectangular channel has been carried out in this paper. The flow is forced to pass over a hot source using a deformable baffle. Different locations of the baffle, power low index and the Richardson number have led to results with the following conclusions.

1. The existence of a deformable (elastic) baffle contributes notable in increasing the average Nusselt number.
2. The location of the deformable baffle that gives maximum Nusselt number is the nearer to the channel inlet part, i.e. upstream of the cavity center.
3. Shear thinning fluid (n < 1) exhibits the largest Nusselt number when Richardson number is greater than unity, whereas the shear thickening (n > 1) experiences the lowest Nusselt values. While for Richardson less or equal to unity, the shear thinning fluid shows the lowest Nusselt number.
4. The best thermal performance of the studied geometry is that when the baffle is located upstream the cavity center i.e. nearer to the exit of the inlet channel.

References

[1] R. P. Chhabra, J. F. Richardson, Non-Newtonian flow and applied rheology: engineering applications, Second Edition, Elsevier, Butterworth-Heinemann, 2011.

[2] H. Xu, S. J. Liao, "Laminar flow and heat transfer in the boundary-layer of non-Newtonian fluids over a stretching flat sheet", Elsevier, Computers & Mathematics with Applications, Vol. 57, No. 9, pp. 1425-1431, 2009.

[3] S. M. Aminossadati, B. Ghasemi, "A numerical study of mixed convection in a horizontal channel with a discrete heat source in an open cavity", Elsevier, European Journal of Mechanics-B/Fluids, Vol. 28, No. 4, pp. 590-598, 2009.

[4] M. T. Islam, S. Saha, M. A. H. Mamun, M. Ali, "Two Dimensional Numerical Simulation of Mixed Convection in a Rectangular Open Enclosure", Fluid Dynamics and Materials Processing, Vol. 4, No. 2, pp. 125-137, 2008.

[5] L. K. Saha, M. C. Somadder, K. M. S. Uddin, "Mixed convection heat transfer in a lid driven cavity with wavy bottom surface", American journal of Applied Mathematics, Vol. 1, No. 5, pp. 92-101, 2013.

[6] M. A. Belmiloud, N. Sad-Chemloul, and M. B. Guemmour, "Influence of the baffle shape on the characteristics of heat transfer in a channel", International Journal of Thermal Technologies, Vol. 6, No. 3, pp. 243-248, 2016.

[7] T. V. Radhakrishnan, G. Joseph, C. Balaji, and S. P. Venkateshan, "Effect of baffle on convective heat transfer from a heat generating element in a ventilated cavity", Springer, Heat Mass Transfer, Vol. 45 pp. 1069-1082, 2009.

[8] M. R. Asif, M. S. Hossain, and K. A. Hossain, "Heat Transfer in a rectangular enclosure with baffles", ARPN Journal of Engineering and Applied Sciences, Vol. 6, No. 4, pp. 29-41, 2011.

[9] S. Sripattanapipat, and P. Promvonge, "Numerical analysis of laminar heat transfer in a channel with diamond-shaped baffles", Elsevier, International Communications in Heat and Mass Transfer, Vol. 36, No. 1, pp. 32-38, 2009.

[10] K. H. Ko and N. K. Anand, "Use of porous baffles to enhance heat transfer in a rectangular channel", Elsevier, International Communications in Heat and Mass Transfer, Vol. 46, No. 22, pp. 4191-4199, 2003.

[11] Y. T. Yang and C. Z. Hwang, "Calculation of turbulent flow and heat transfer in, different aspect ratio channels and different porosity baffles were used porous-baffled channel", Elsevier, International Communications in Heat and Mass Transfer, Vol. 46, No.5, pp. 771-780, 2003.

[12] M. Yilmaz, "The effect of inlet flow baffles on heat transfer", Elsevier, International Communications in Heat and Mass Transfer, Vol. 30, No. 8, pp. 1169-1178, 2003.

[13] Y. L. Tsay, J. C. Cheng and T. S. Chang, "Enhancement of heat transfer from surface-mounted block heat sources in a duct with baffles", Numerical Heat Transfer, Part A, Vol. 43, No. 8, pp. 827-841, 2003.

[14] B. C. Feijó, G. Lorenzini, L. A. Isoldi, L. A. O. Rocha, J. N. V. Goulart, and E. D. Dos Santos. "Constructal design of forced convective flows in channels with two alternated rectangular heated bodies", Elsevier, International Journal of Heat and Mass Transfer, Vol. 125, pp. 710-721, 2018.

[15] M. Najam, A. Amahmid, M. Hasnaoui and M. El Alami, "Unsteady mixed convection in a horizontal channel with rectangular blocks periodically distributed on its lower wall", International Journal of Heat and Fluid Flow, Vol. 24, No. 5, pp. 726-735, 2003.

[16] A. Korichi and L. Oufer, "Numerical heat transfer in a rectangular channel with mounted obstacles on upper and lower walls", International Journal of Thermal Science, Vol. 44, No. 7, pp. 644-655, 2005.

[17] A. Korichi and L. Oufer, "Heat transfer enhancement in oscillatory flow in channel with periodically upper and lower walls mounted obstacles", International Journal of Heat and fluid flow, Vol. 28, No. 5, pp.1003-1012, 2007.

[18] X. Sun, Y. Zehua, L. Jiajun, K. Wen and H. Tian, "Forced convection heat transfer from a circular cylinder with a flexible fin", Elsevier, International Journal of Heat and Mass Transfer, Vol. 128, pp. 319-334, 2019.

[19] M. Vera and A. Linan, "Laminar counter flow parallel-plate heat exchangers: exact and approximate solutions", Elsevier, International Journal of Heat and Mass Transfer, Vol. 53, No. 21-22, pp. 4885-4898, 2010.

[20] C. Kang and K. S. Yang, "Heat Transfer Characteristics of Baffled Channel Flow", Journal of Heat Transfer, Vol. 133, No. 9, 2011.

[21] C. C. Wang, W. L. Fu and C. T. Chang, "Heat transfer and friction characteristics of typical wavy fin-and-tube heat exchangers", Elsevier, Experimental thermal and fluid science, Vol. 14, No. 2, pp. 174-186, 1997.

[22] C.C. Wang, J.Y. Jang and N. F. Chiou, "A heat transfer and friction correlation for wavy fin-and-tube heat exchangers", International Journal of Heat and Mass Transfer, Vol. 42, No. 10, pp. 1919-1924, 1999.

[23] A. K. Sharma, P. S. Mahapatra, N. K. Manna and K. Ghosh, "Mixed convection in a baffled grooved channel", Springer, Sadhana, Vol. 40, pp. 835-849, 2015.

[24] M. A. Ismael, "Forced convection in partially compliant channel with two alternated baffles", International Journal of Heat and Mass Transfer, Vol. 142, pp. 118455, 2019.

[25] R. Abdi, N. Rezazadeh and M. Abdi, "Investigation of passive oscillations of flexible splitter plates attached to a circular cylinder", Journal of Fluids and Structures, Vol. 84, pp. 302-317, 2019.

[26] M. Ghalambaz, E. Jamesahar, M. A. Ismael and A. J. Chamkha, "Fluid-structure interaction study of natural convection heat transfer over a flexible oscillating fin in a square cavity", International Journal of Thermal Sciences, Vol. 111, pp. 256-273, 2017.

[27] D. Chakraborty, J. R. Prakash, J. Friend and L. Yeo, "Fluid-structure interaction in deformable microchannels", Physics of Fluids, Vol. 24, pp. 102002, 2012.

[28] S. P. Rajesh and Valluru, "Design and analysis of fluid structure interaction for elbow shaped micro piping system", Excerpt from Proceedings of the 2014 COMSOL Conference in Bangalore.

[29] F. X. Tanner, A. A. Al-Habahbeh, K. A. Feigl, S. Nahar and S. A. K. Jeelani, W.R. Case and E. J. Windhab, "Numerical and experimental investigation of a non-Newtonian flow in a collapsed elastic tube", Applied Rheology, Vol. 22, No. 6, pp. 63910, 2012.

[30] S. Nahar, S. A. K. Jeelani, E. J. Windhab, "Influence of elastic tube deformation on flow behavior of a shear thinning fluid", Elsevier, Chemical Engineering Science, Vol. 75, No. 18, pp. 445-455, 2012.

[31] J. Donea, S. Giuliani and J. P. Halleux, "An arbitrary Lagrangian-Eulerian finite element method for transient dynamic fluid-structure interactions", Elsevier, Computer methods in applied mechanics and engineering, Vol. 33, No. 1-3, pp. 689-723, 1982.

Biographies

Duna Tariq Yaseen received B.Sc. degree Mechanical Engineering from Dept. of Mechanical Engineering, College of Engineering, University of Basrah, Basrah, Iraq in 1990. She received the M.Sc. degree in Applied Mechanics from University of Basrah, Basrah, Iraq in 2014. She worked as technical instructor in the Dept. of power Mechanics Techniques, Basrah Technical Institute, South Technical University, Basrah, Iraq from 1992 to 2012. She rejoined the same department as assistant lecturer from 2014 to 2016. Currently she is a Ph.D. student in the mechanical engineering department, college of engineering university of Basrah, Basrah, Iraq. Working in the field of fluid flow.

Muneer A. Ismael received B.Sc., M.Sc. and Ph.D. degrees from University of Basrah, Basrah, Iraq, in 1996, 1998 and 2007, respectively. He is currently Professor in the Mechanical Engineering Department at the University of Basrah, Iraq. In his postgraduate projects, he worked on designing the electromagnetic flowmeter for partially filled pipes. His research interests included numerical modeling, porous media, convective heat transfer, nanofluid, and flow measurements.